Article

Delaying the Occurrence of Bar Buckling in RC Columns Confined with SRG Jacketing

Georgia E. Thermou [1,*] and Sousana Tastani [2,*]

1   Civil Engineering Department, The University of Nottingham, Nottingham NG7 2RD, UK
2   Civil Engineering Department, Democritus University of Thrace, 67100 Xanthi, Greece
*   Correspondence: georgia.thermou@nottingham.ac.uk (G.E.T.); stastani@civil.duth.gr (S.T.)

Abstract: This paper investigates experimentally the structural performance of substandard reinforced concrete (RC) short columns confined with steel-reinforced grout (SRG) jackets under monotonically increasing uniaxial compression. The study comprised 24 square cross section short RC columns having alternative arrangements of shear reinforcement (ratio of stirrup spacing to longitudinal bar diameter ranging from 4.2 to 12.5). The short columns were retrofitted with externally applied SRG jacketing differing by the density of the fabric (4 cords/in and 12 cords/in) and the number of fabric layers (1 and 2). The test results showed that retrofitting significantly changed the behaviour of the specimens compared to the unconfined counterparts. For columns at risk of premature failure due to insufficient support of compression bars provided by the sparse stirrups, the SRG jackets delayed bar buckling, enabling the members to achieve greater strength and deformation capacity. The well-detailed specimens helped establish the maximum effectiveness of SRG confinement.

Keywords: steel-reinforced grouts; confinement; buckling; seismic strengthening

1. Introduction

Reinforced concrete (RC) critical structural elements (columns/beams) that do not conform to modern codes for seismic resistance introduced in the early 1980s are characterized by inferior material quality (concrete compressive strength less than 20 MPa, steel yielding stress lower than 400 MPa) and inadequate transverse reinforcement detailing. Especially, columns' areas of high moment and axial load demands due to seismic excitations (plastic hinge regions) suffer large inelastic deformations, which with the absence of dense and well anchored stirrups undergo quick deterioration of strength [1]. Especially for the transverse reinforcement used in construction practices before the 1980s in South Europe, it typically consists of smooth bars as small as 5 mm in diameter, with their ends simply overlapping at the corners. These stirrups are sparsely placed, resulting in a maximum spacing s_{max} = min[min{b, h}, 12D_b], where b and h are the dimensions of the cross section, and D_b is the diameter of the longitudinal reinforcement bars. For example, for b = h = 300 mm and D_b = 14 mm, then s_{max} equals 168 mm (refer to Chapter 4 in [1]) which means that only a single stirrup's legs cross a potential diagonal crack with nil contribution to shear resistance of a column under seismic excitation. Moreover, this lack of appropriate size and arrangement of stirrups leads to a significant unsupported length of the compressive longitudinal reinforcing bars, making them susceptible to buckling when reversed seismic sway induces increased axial loads to columns. As a consequence, there is an increased risk of brittle failure in the structural element because it possesses inadequate resistance to reversed cyclic load. The safe performance of the entire building can be compromised by localized damage in the plastic hinge regions of the columns, where sideways buckling of the compression reinforcement is expected due to the lateral shear distortion in that area.

Mainly, the slenderness ratio s/D_b [2–6] along with the stiffness and the anchorage detailing of the stirrups play a key role in the stability of compression reinforcing bars. The

slenderness ratio s/D_b could range between 6 and 8 in case of high to moderate ductility RC members [7], whereas for s/D_b lower than 5 ($s/D_b < 5$), the bar in compression is able to develop its full strain–strain response as in the case of tension. For values higher than eight ($s/D_b > 8$), the bars could reach buckling state when their compressive stress reaches yielding point [5,6]. According to the practice detailing of the pre-1970s era, s/D_b could receive any value between 10 and 40 [7].

The beneficial impact of confinement on the compressive behaviour of substandard RC columns has been consistently observed in previous studies [6–13]. External wrapping using either FRP (fibre-reinforced polymers) or TRM (textile-reinforced mortars) has been found to increase the axial compressive strength and associated strain ductility. This improvement is attributed to the prevention of premature buckling of the reinforcing bars, delaying it to occur at higher levels of strain ductility [8,12]. When the longitudinal reinforcement approaches a state of instability at the critical axial strain, the bar undergoes lateral bending to maintain compatibility with the increasing axial strain of the supporting concrete core [4]. By wrapping the column with composite fabrics, the confined concrete experiences enhanced strength and strain capacity. As long as the increased axial strength of concrete due to confinement is able to undertake the overload released by the buckled reinforcement, the member continues to deform until strain concentrations limit the effectiveness of the composite jacket as lateral support for the longitudinal reinforcement [12].

Steel-reinforced grout (SRG) jacketing presents an alternative composite system that combines high-strength steel-reinforced fabric with cementitious grout [14], appropriate for strengthening techniques of RC deficient structures [15–18]. Previous studies focusing on uniaxial compression of SRG-confined plain and reinforced concrete have provided evidence of the system's effectiveness in enhancing both axial strength and associated deformation capacity [19–22]. Aiming to enhance the limited data as per this type of strengthening configuration, the effectiveness of SRG jackets of axially compressed, lightly reinforced RC columns (with s/D_b ratios equal to 12.5 and 6.25) was experimentally investigated and compared with well-detailed SRG counterparts ($s/D_b = 4.17$) corresponding to the highest confinement that can be offered by SRG jacketing. The specimens were designed as to be susceptible to rebar buckling failure with the compression reinforcing bars losing their stability upon yielding. Single- or double-layered SRG jacket configurations were applied to 18 square cross section columns, whereas 6 more were used as control specimens. The experimental results show that the SRG jackets increased substantially the axial strength and deformation capacity, thus upgrading the structural element performance to be conformable to the requirements of modern codes for seismic resistance. The analysis of the data through a simple mechanistic model shows that the lateral confining pressure exerted by the jackets provided to the concrete core the required axial strength reserves to be able to undertake the load release by the compressive reinforcement upon attainment of unstable conditions. This strength reserve along with the jacket strain reserve at corners enables the structural component to increase its compressive strain ductility (sustaining of strength with increasing strain), thus delaying bar buckling failure to occur at higher compressive strain level.

Research Significance

The design methodology for retrofitting substandard RC columns with FRP jacketing has been extensively established in [23]. In recent developments, there has been a transition from using polymeric binders to inorganic binders (shifting from FRPs to TRMs) to develop an environmentally friendly system and to mitigate issues such as degradation due to ultraviolet radiation and temperature-induced resin softening. Furthermore, the substitution of carbon fibre with steel fibre (progressing from TRMs to SRGs) has been explored, aiming to achieve a more cost-effective and fire-resistant jacketing system. This experimental investigation is carried out aiming to assess the effectiveness of several SRG jacketing configurations in delaying bar buckling in columns representative of older construction practice to occur at increased levels of deformation capacity. Additionally, the

design expressions outlined in chapter 8 of [23] are implemented to predict the performance of SRG confined columns.

2. Experimental Program

2.1. Design of Specimens and Parameters of Investigation

A total of 24 short RC columns of 200 mm square cross section and of 320 mm in height were tested in uniaxial compression. The specimen geometry was dictated by former studies of the authors [22] along with the restrictions imposed by the loading frame machine. Thus, a 1:2 scale of an actual column was chosen. The edges of all specimens were rounded off by a corner radius r = 25 mm aiming to facilitate the best practice of SRG jacketing (a precaution step before casting, Figure 1). The longitudinal reinforcement comprised four bars of diameter D_b = 12 mm [$\rho_l = 4 \times \pi \times D_b^2/(4 \times 200^2)$ = 1.13%] placed at the corners of the specimens as shown in Figure 1. The clear cover of the steel gage was 20 mm. Three transverse reinforcement arrangements were used corresponding to 6 mm diameter stirrups: two with their ends bent at 90°, spaced at s = 150 mm (s/D_b = 12.5) and at s = 75 mm (s/D_b = 6.25) referring to old practice and one with tie ends bent at 135° and spaced at s = 50 mm (s/D_b = 4.2) referring to concurrent code requirements. An additional 8 mm stirrup (tie ends bent at 135°) was placed at the specimen ends, near the loading surfaces, aiming to prevent local crushing of concrete and to drive failure into the region under study.
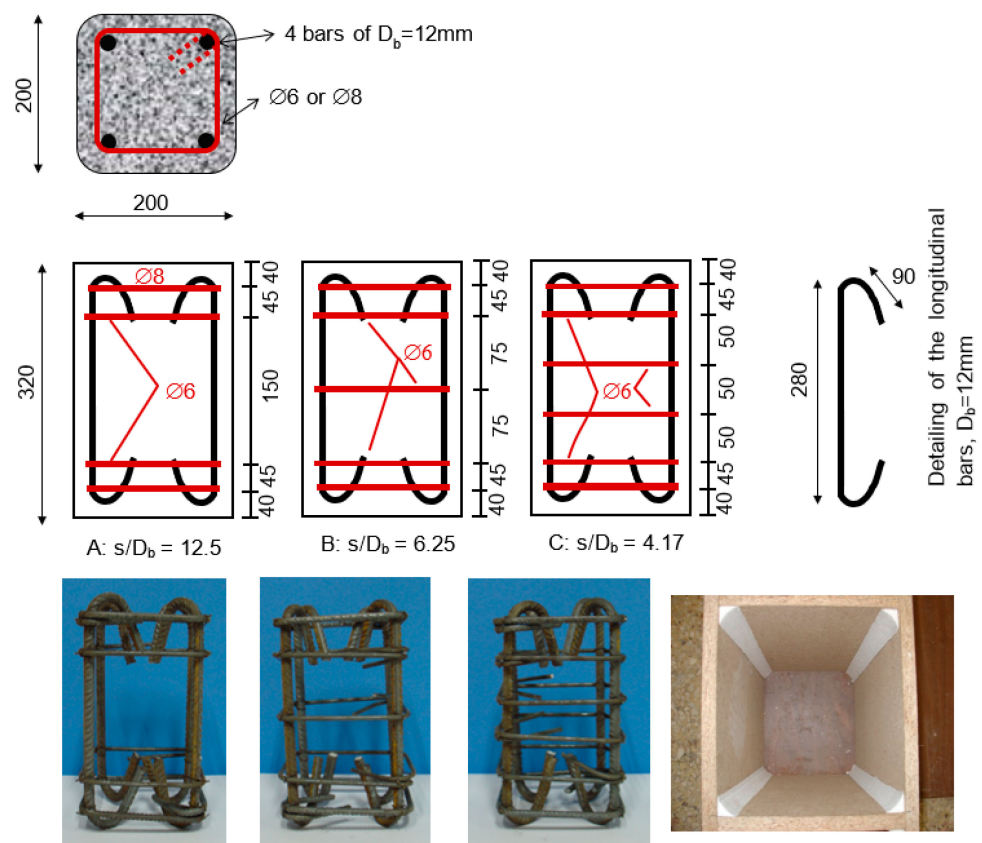

Figure 1. Geometry and reinforcement detailing of the columns (dimensions in mm), steel cages of the three groups of specimens and mould with rounded corners.

Based on the stirrups' arrangement, the specimens were divided into three groups: Group A with s/D_b = 12.5, Group B with s/D_b = 6.25 and Group C with s/D_b = 4.17 (Table 1). Six columns (two from each group) served as the control specimens whereas the rest (eighteen in total, six from each group) were retrofitted by three different SRG jacketing configurations depending on the number of layers and steel textile density (cords/in) as

follows: (i) one layer of 4 cords/in, (ii) two layers of 4 cords/in and (iii) two layers of 12 cords/in density steel textile. The notation of the specimens is as follows: X denotes the group of the unconfined specimens (A, B or C); for the rest SRG jacketed columns, the notation DjX applies, where D indicates the density of the fabric with L (light) and H (high) for the 4 and 12 cords/in textiles, respectively; j refers to the number of layers (1 or 2); and X corresponds to the group name of the specimens (A, B or C). Two identical specimens were tested for each configuration. The specimen details appear in Table 1.

Table 1. Specimen details.

Specimen Notation	Group	Fabric Density: (Cords/in) L = 4 or H = 12	Layers
A	A s/D_b = 12.5 tie ends bent at 90°	-	-
L1A		4	1
L2A		4	2
H2A		12	2
B	B s/D_b = 6.25 tie ends bent at 90°	-	-
L1B		4	1
L2B		4	2
H2B		12	2
C	C s/D_b = 4.17 tie ends bent at 135°	-	-
L1C		4	1
L2C		4	2
H2C		12	2

2.2. Material Properties

The same concrete mix was used for all specimens. Nine standard cylinders (150 × 300 mm) were cast for obtaining the average compressive strength at the day of the tests. The average compressive strength was f_{cm} = 28.7 MPa (SDV = 0.74), corresponding to a characteristic compressive strength of C20/25 (f_{ck} = f_{cm} − 8 MPa) which is almost the same as B25 [1], i.e., a good quality concrete for the construction practice before the 1980s.

The 12 mm diameter ribbed bars had a yield stress of f_{sy} = 540 MPa, ultimate stress f_{su} = 640 MPa, strain at the initiation of hardening ε_h = 0.005 and at fracture ε_u = 0.1, corresponding to steel quality BStIV [1] used in seismic applications in the 1970s. The 6 mm diameter smooth bar reinforcement used for the stirrups had a yield stress of f_{sy} = 360 MPa and an ultimate stress f_{su} = 467 MPa. These values correspond to BStI, which was used extensively for shear reinforcement [1].

The 3X2 unidirectional ultra-high strength steel textile was utilized for the fabrication of the SRG jackets. The term 3X2 denotes that each cord is made by twisting five wires, three straight and two wrapped with a high torque angle to enhance the interlocking with the mortar (Figure 2). The cords are thermo-welded to a fibreglass micromesh and galvanized (coated with zinc) to improve durability in a chloride, freeze-thaw and high humidity environment. Each cord has an area of 0.538 mm², a tensile strength higher than 2800 MPa, a strain to failure higher than 0.015 and an elastic modulus higher than 190 GPa. The textiles used had a density of 4 cords/in (1.57 cords/cm) and 12 cords/in (4.72 cords/cm) (Figure 2). The equivalent thickness per unit width, t_s, for the 4 cords/in and the 12 cords/in was defined equal to 0.084 mm (=0.538 mm²/cord × 1.57 cords/10 mm) and 0.254 mm, respectively. The axial stiffness (=190 GPa × t_s × n, n the number of plies) of the SRG jacket configurations applied (with reference to the periphery of the column) was 15,960 N/mm for the 4 cords/in single jacket (t_s = 0.084 mm, n = 1), 31,920 N/mm for the

4 cords/in two-layered jacket (t_s = 0.084 mm, n = 2) and 96,520 N/mm for the 12 cords/in two-layered jacket (t_s = 0.254 mm, n = 2).
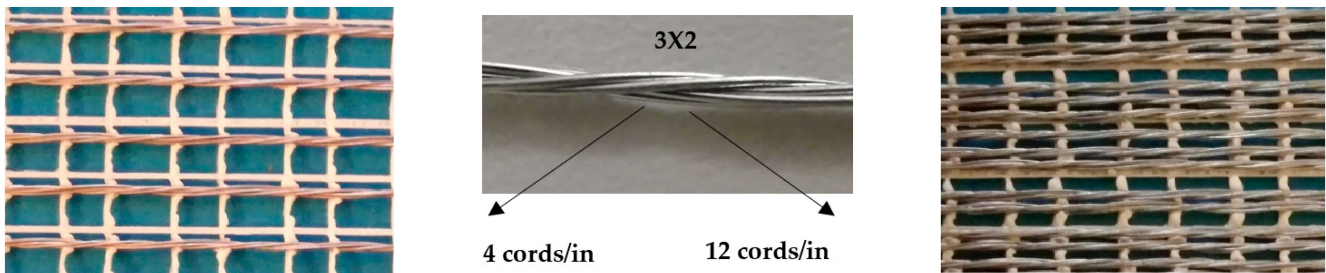

Figure 2. Unidirectional ultra-high strength steel textile.

The grout used for the SRG composite system was a commercial mortar with a crystalline reaction geobinder base and a very low petrochemical polymer content and free from organic fibres. The mortar was utilised as the substrate material applied to the concrete surface of the specimens, the bonding material between the applied layers of the steel fabric and as a final cover. Its reported mechanical properties at 28 days are as follows: modulus of elasticity E_m = 25 GPa; flexural strength f_{mf} = 10 MPa; compressive strength f_{mc} = 55 MPa; and adhesive bond f_{mb} = 2 MPa. According to former studies [24,25] the composite SRG in direct tension may develop a bilinear response with the second branch of lower modulus (lower than 2/3 of the Modulus of Elasticity of cord) and a strain capacity up to 0.025 (which is higher than the limit strain 0.015 given by the manufacture); this upper strain limit ε_{ju} = 0.025 is considered later in Section 4 as a reference point for the lateral response of the SRG columns aiming to explore the strain capacity of the SRG jacket as a function of bar buckling.

2.3. Strengthening Procedure

The first step of the strengthening procedure is the roughening of the specimens' surface aiming to enhance the friction between the concrete substrate and the SRG system. After cleaning and saturating the substrate, the grout was applied manually onto the lateral surface of the specimens (Figure 3). The steel textiles were pre-bent considering the corner radius (r = 25 mm) to facilitate the application procedure (Figure 3). The height of the steel textile was 300 mm (leaving an uncovered portion of 10 mm at the top and bottom of the specimens). The grout was squeezed out between the steel fibres by applying pressure manually (Figure 3). After the application of the textile to one full-perimeter (or two in the case of two-layered jacket), the required overlap length was decided to be equal to two sides aiming to preclude unfavourable debonding. More specifically, the estimated mortar bond strength per unit width (=bond strength times the length of two cross section sides = $f_{mb} \times 2 \times 200$ mm = 800 N/mm) is greater than the nominal tensile strength of the outer SRG layer (i.e., for L1/L2 is $1 \times 0.084 \times 190{,}000 \times 0.015 = 240$ N/mm and for the H2 is $1 \times 0.254 \times 190{,}000 \times 0.015 = 720$ N/mm). In real applications the bond conditions could be further enhanced by also applying mechanical anchorage. A final coat of the cementitious grout was applied to the exposed surface. The total thickness of the SRG jacket was 7 mm and 10 mm for the single- and double-layered, respectively; hence, the geometry of the jacketed specimens was slightly affected (up to 5% increase of the side size). The application of the high-density (H) and high-stiffness jacket (two-layered) imposed difficulties (especially for the second layer) regarding, i.e., the penetration of the mortar through the textile and the fitting at the rounded corners of the column.

Figure 3. Steps of the SRG jackets application.

2.4. Test Setup

The specimens were subjected to monotonically increasing concentric uniaxial compression load up to failure, and both axial and lateral strains were measured (Figure 4). The loading was applied at a rate of 0.15 MPa/s in load control, using a 6000 kN compression testing machine. The axial strain was calculated using the measurements of four linear variable differential transducers (LVDTs) mounted on the four sides of the specimens with the help of two custom made metallic frames attached symmetrically to the end regions of the specimen (Figure 4). The per center distance between the two frames was 200 mm (this is also the gauge length of the LVDTs for the definition of the axial strain). The lateral strain of the column mid height cross section and at the middle of each side was measured by four LVDTs. The axial load was measured from a load cell placed at the top of the specimen and converted to stress by dividing with the cross section area (200×200 mm^2) (Figure 4).
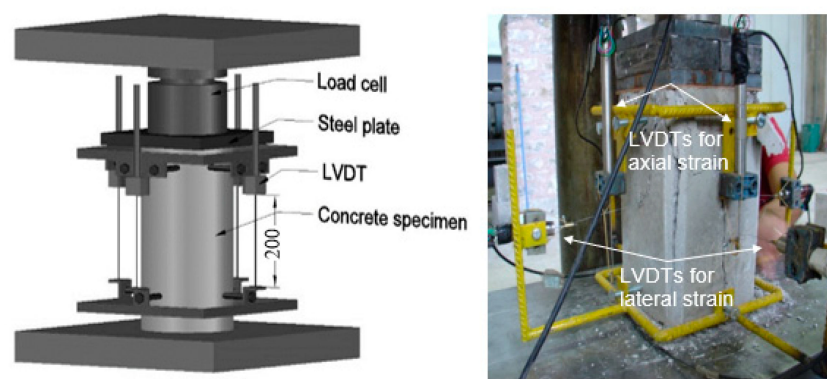

Figure 4. Test setup and position of LVDTs for axial and lateral strain measurements.

3. Test Results and Discussion

3.1. Failure Modes

The control specimens A and B with bar slenderness ratios $s/D_b = 12.5$ and $s/D_b = 6.25$, respectively, and insufficient tie ends bend at 90° failed abruptly in the middle-height region due to symmetrical buckling of the longitudinal reinforcing bars (Figure 5, specimens labelled as A, B). Specimens C with $s/D_b = 4.17$ and tie end bend at 135° developed a more ductile mode of failure without excessive signs of outwards bending of the longitudinal reinforcing bars (Figure 5).

The majority of the SRG jacketed columns failed at advanced state of axial deformation associated by inelastic bar buckling. Rupture of the cords occurred mostly at the middle height of the specimens with progressive debonding of the textile at the anchorage zone. In the specimens confined by two-layered SRG jackets, rupture of the cords was observed in both layers. In general, the addition of the SRG jackets in the columns, especially in those of high slenderness ratios ($s/D_b \geq 6.25$), postponed bar buckling of the longitudinal reinforcement to occur at higher levels of axial deformation.

Figure 5. Control (X = A, B, C) and SRG-jacketed columns (DiX) at failure.

3.2. Response under Monotonic Axial Load

The axial stress versus axial/lateral strain response curves of the tested columns per group are presented in Figure 6, aiming to demonstrate the influence of the increased jacket stiffness (from lighter to darker colour in each diagram) to a specific bar slenderness ratio s/D_b (green-coloured curves correspond to $s/D_b = 12.5$; blue-coloured curves correspond to $s/D_b = 6.25$; and orange coloured curves correspond to $s/D_b = 4.17$). In general, it is observed that as the SRG stiffness increases, both axial strength and axial deformation capacity (here considered the deformation beyond which an abrupt reduction of strength occurs) increase for all three stirrup arrangements. Additionally, the lateral deformation capacity, which may quantify the confining pressure provided by the SRG jacket and accounts for concrete core dilation and stretching due to outwards bending of the bars, increases as the bar slenderness ratio (s/D_b) decreases (Figure 6). All control columns developed similar strength (around 30 MPa, which coincides with the cylinder concrete compressive strength) regardless of the s/D_b value. However, their axial deformation capacity increased as the s/D_b decreased. The vertical dashed line in Figure 6 denotes the upper strain limit of an SRG system in direct tension (i.e., 0.025 according to [24–26]). This limit is compared with the experimental lateral strain values at the initiation of strength drop for each specimen (see values $\varepsilon_{lat,cc}$ in column (4) of Table 2). Since the recorded values often exceed the established limit value (i.e., 0.025 [24–26]) by a significant margin, it has been decided not to use these data in the analysis. However, for the sake of completeness, they are presented here.
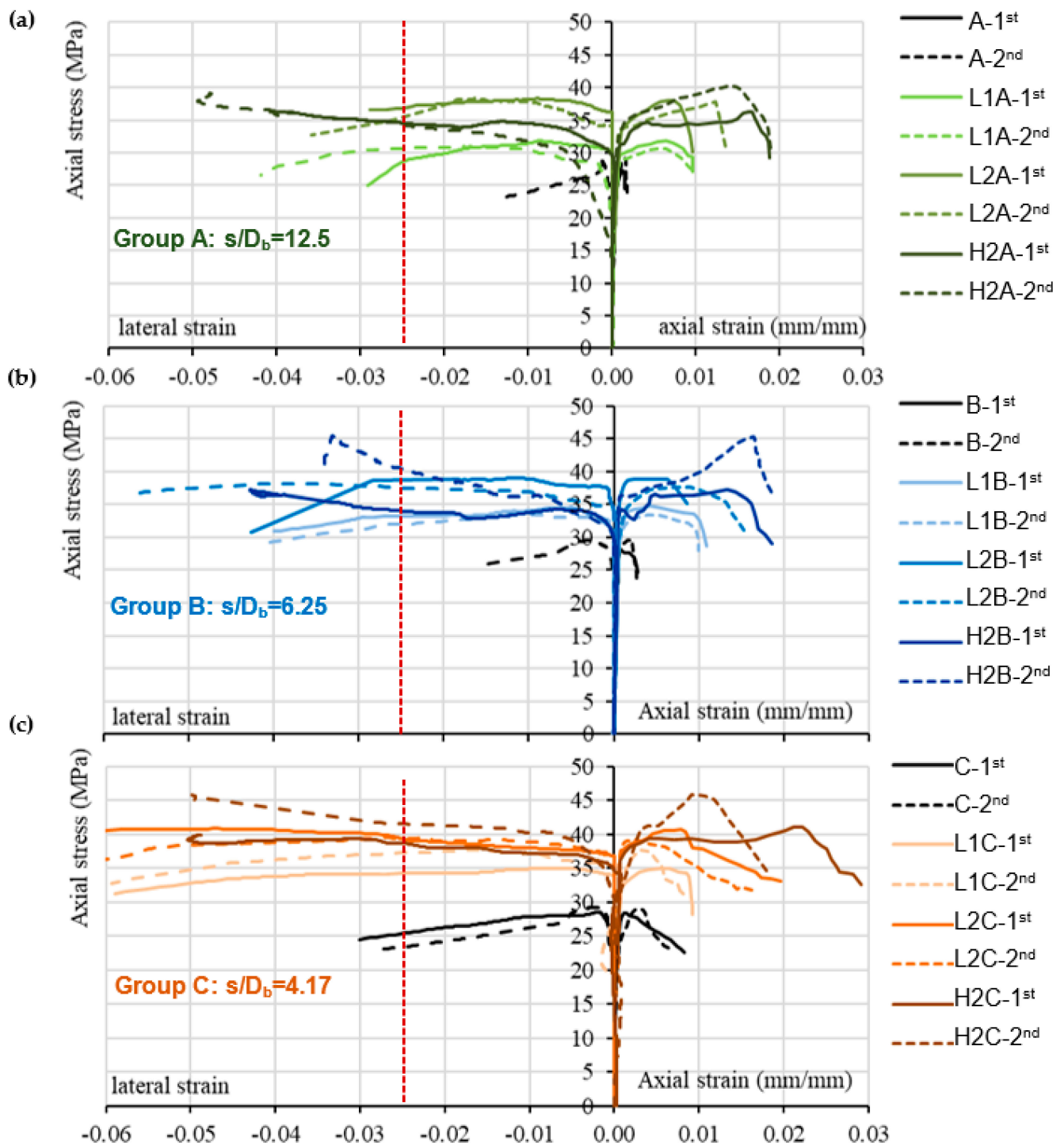
Figure 6. Axial stress–axial/lateral strain curves of the tested columns of (**a**) group A (s/D$_b$ = 12.5); (**b**) group B (s/D$_b$ = 6.25); (**c**) group C (s/D$_b$ = 4.17).

Table 2. Test results of columns.

Name	f_{cc} (MPa)		ε_{cc}		$\varepsilon_{lat,cc}$		ε_{ccu}		f_{cc}/f_o %	$\varepsilon_{cc}/\varepsilon_y$ #	$\varepsilon_{ccu}/\varepsilon_y$ #
	Value	Mean	Value	Mean	Value	Mean	Value	Mean	Mean	Mean	Mean
(1)	(2)		(3)		(4)		(5)		(6)	(7)	(8)
A-1st	27.2	28.2	0.0015	0.0016			0.0015	0.0016	0.97	0.64	0.64
A-2nd	29.2		0.0017				0.0018				
L1A-1st	31.9	31.2	0.0070	0.0065	0.009	0.011	0.0098	0.0098	1.08	2.60	3.93
L1A-2nd	30.6		0.0060		0.013		0.0098				
L2A-1st	38.0	37.9	0.0080	0.010	0.011	0.014	0.0097	0.0116	1.31	4.00	4.66
L2A-2nd	37.8		0.0120		0.017		0.0136				
H2A-1st	36.3	38.3	0.0160	0.0155	0.040	0.045	0.0188	0.0184	1.32	6.20	7.37
H2A-2nd	40.3		0.0150		0.050		0.0180				
B-1st	28.3	29.0	0.0025	0.0023			0.0028	0.0027	1.00	0.92	1.10
B-2nd	29.7		0.0021				0.0027				
L1B-1st	34.7	34.0	0.0060	0.006	0.012	0.012	0.0109	0.0105	1.17	2.4	4.19
L1B-2nd	33.4		0.0060		0.012		0.0100				
L2B-1st	38.8	38.2	0.0080	0.009	0.028	0.034	0.0086	0.0113	1.22	3.52	4.52
L2B-2nd	37.6		0.0100		0.040		0.0140				
H2B-1st	37.3	41.3	0.0130	0.0145	0.042	0.037	0.0160	0.0165	1.42	5.80	6.60
H2B-2nd	45.4		0.0160		0.032		0.0170				
C-1st	28.4	28.7	0.0029	0.0032			0.0060	0.0062	0.99	1.26	2.47
C-2nd	29.1		0.0034				0.0063				
L1C-1st	35.0	36.3	0.0065	0.0053	0.030	0.038	0.0090	0.0083	1.12	2.10	3.30
L1C-2nd	37.6		0.0040		0.045		0.0075				
L2C-1st	40.7	39.9	0.0085	0.0073	0.050	0.055	0.0150	0.0130	1.38	2.90	5.20
L2C-2nd	39.2		0.0060		0.060		0.0110				
H2C-1st	41.1	43.5	0.0220	0.0170	0.050	0.05	0.0260	0.0205	1.50	6.80	8.20
H2C-2nd	45.8		0.0120		0.050		0.0150				

% f_o is the concrete strength (29 MPa); # ε_y = 0.0025 is the yielding strain of the compression reinforcement; it is considered in order for the ε_{cc} and ε_{ccu} values to be compared highlighting the influence of bar slenderness effect.

Figure 7a–c depict how effective a particular jacket configuration is in increasing the strength and deformation capacity with progressive improvement of the longitudinal bars support conditions, i.e., by lowering the s/D_b ratio (the same colour code is used as in in Figure 6). Note that all unconfined columns developed the same strength regardless of the s/D_b ratio. The single-layered 4 cords/in density SRG jackets slightly improved the strength (up to 15% in comparison the control specimens which was close to 30 MPa) but kept the axial deformation capacity at the same level with decreasing s/D_b (Figure 7a). The two-layered 4 cords/in density SRG jackets increased the strength by the same level (around 38 MPa, corresponding to 25% compared to the value of the control specimen) but of higher axial deformation in case of s/D_b = 4.17 (Figure 7b). The two layered 12 cords/in SRG jacket improved the strength (increase of 25% to 40% in comparison to 30 MPa in the control specimens) by sustaining the axial deformation to similar levels as s/D_b decreased (Figure 7c).
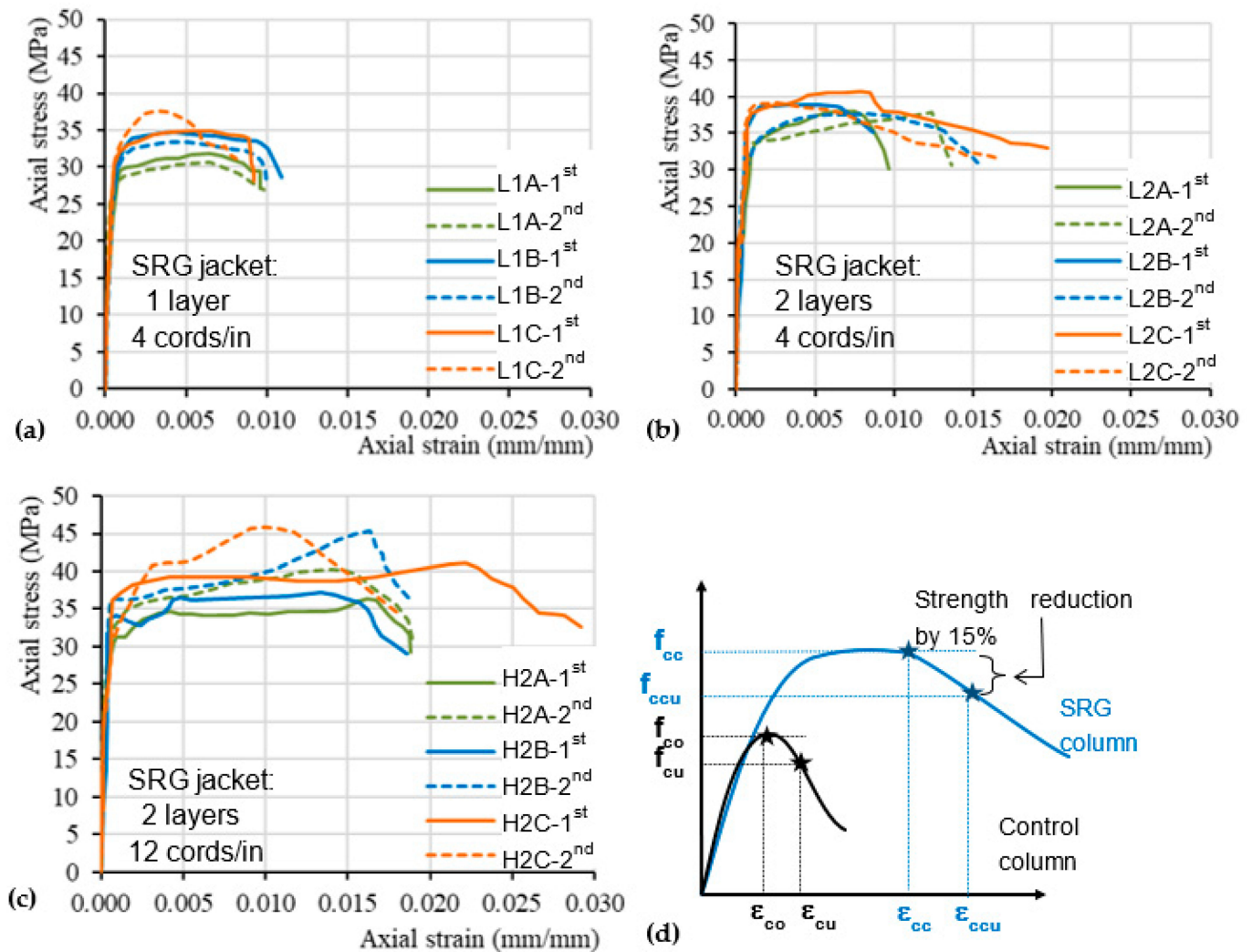
Figure 7. Axial stress–strain curves of the tested SRG jacketed columns; (**a**) 1 layer–4 cords/in; (**b**) 2 layers–4 cords/in; (**c**) 2 layers–12 cords/in. (**d**) Nomenclature for the axial stress–strain milestone points.

An interesting observation is that the axial stress–strain response for most of the SRG-jacketed columns (Figure 7) is characterized by a horizontal plateau at strength, although the steel textile has an elastic behaviour up to rupture (like to FRP fabrics). This may be attributed to the elastoplastic bond–slip law of the SRG, which presents a wide plateau at bond strength between slip values 0.1–0.5 mm, and the upper limit further increases up to 1 mm with bonded length over 200 mm [25,26]. The corresponding bond–slip law of the FRP usually has a parabolic shape that terminates at slip of 0.2–0.3 mm [27]. The variation in bond response between the SRG and FRP jacketing systems potentially explains why the SRG jacket enables plastic response under axial compression, whereas the FRP jacket results in a hardening branch following elastic response [12,28].

The test data are analysed for two limit states of response as defined in Figure 7d and are summarized in Table 2. The first state corresponds to the strength beyond which a descending branch initiates (columns (2–3) in Table 2); point (f_{co}, ε_{co}) for the control specimens and point (f_{cc}, ε_{cc}) for the confined ones in Figure 7d. The lateral strain $\varepsilon_{lat,cc}$ is also defined at this level (column (4) in Table 2). The second state corresponds to the ultimate state which is defined at 15% drop of strength (column (5) in Table 2); points (f_{cu}, ε_{cu}) and (f_{ccu}, ε_{ccu}) for the control and SRG confined columns, respectively. The proximity of the two states denotes how abruptly the strength degradation occurs. Column (6) denotes the increased strength of the SRG-jacketed columns as compared with the concrete strength

(f_o = 29 MPa). Columns (7–8) present the ratios of the axial strain at strength and at ultimate deformation to the yielding strain ε_y = 0.0025 of the compression reinforcement. The selection of ε_y instead of ε_{co} aims to highlight the influence of the bar slenderness to the abrupt failure of the control columns (values lower than 1 in cases A and B of s/D_b = 12.5 and 6.25, respectively). The term $\varepsilon_{ccu}/\varepsilon_y$ represents the compression ductility μ (=$\varepsilon_{ccu}/\varepsilon_y$). As seen in Table 2, for the SRG columns, the average strength increase ($f_{cc}/f_o - 1$) and μ values range from 10% to 50% and from 3 to 8, respectively.

4. Analysis of the Axial and Lateral Response Due to SRG Confinement

The context of Chapter 8 of the fib Bulletin 90 [23] for FRP-jacketing design is adopted here aiming to examine its appropriateness in case of SRG jacketing.

4.1. Axial Response Indices

The average confining pressure exerted by the SRG-jacketing system when applied to RC members is obtained as the average lateral stress developing in the two principal directions of the cross section. Similar to the FRP jacketing [8,23,29], the average confining pressure is

$$\sigma_{lat} = \frac{1}{2}\left(\underbrace{\alpha^{SRG}\rho_v^{SRG}E_f\varepsilon_{j,eff}}_{SRG\ \text{confinement}} + \underbrace{\alpha^{st}\rho_v^{st}f_y^{st}}_{stirrup\ \text{confinement}} \right) \tag{1}$$

The first and second part of Equation (1) correspond to the contribution of the SRG jacket and stirrups, respectively. Term E_f is the modulus of elasticity of steel cord (i.e., 190 GPa), and ε_{eff} is the effective tensile strain the jacket develops. The volumetric ratios ρ_v^i of the transverse reinforcements are as follows: for the SRG ρ_v^{SRG} = $2nt_s(b+h)/(bh)$ where n is the number of layers and t_s is the equivalent layer thickness per unit width (see Section 2.2) and b, h are the cross section sides (i.e., here b = h = 200 mm); for stirrups ρ_v^{st} = $A_{st}(b_o+h_o)/(b_oh_os)$ where A_{st} is their total sectional area (i.e., here $2 \times \pi \times 6^2/4$ = 56.5 mm²) and b_o, h_o the confined core dimensions [i.e., here $b_o = h_o = 200 - 2 \times (c + D_{st})$ = 148 mm]. The term α^i is the confinement effectiveness factor of the transverse reinforcement; for the SRG jacket α^{SRG} = 0.63 as it is defined by Equation (A1) in Appendix A [23]. The term α^{st} defined according to EC8-Part I [30] is calculated equal to 0.07, 0.16, 0.19 for the ∅6/150, ∅6/75 and ∅6/50 stirrups respectively.

The confined concrete strength f_{cc} and the corresponding strain ε_{cc} are calculated from the confinement model of Richart et al. [31] as follows (f_o is the unconfined concrete strength):

$$f_{cc} = f_o + 3\sigma_{lat} \tag{2}$$

$$\varepsilon_{cc} = 0.002\left(1 + 15\frac{\sigma_{lat}}{f_o}\right) \tag{3}$$

The failure strain of confined concrete, ε_{ccu}, corresponding to a compression strength reduction in excess of 15% is obtained from [23]:

$$\varepsilon_{ccu} = 0.0035 + 0.075\left(\frac{2\sigma_{lat}}{f_c} - 0.1\right) \geq 0.0035 \tag{4}$$

Equations (1) and (2) are used to predict the deformation indices measured during the testing procedure. From Equation (2), lateral pressure σ_{lat} is estimated by using f_{cc} values from column (1) of Table 3 and f_o = 29 MPa. The term σ_{lat}/f_o shown in column (4) of Table 3 represents a measure of the confining pressure magnitude provided by the SRG jacket as per the unconfined concrete strength; it ranges from 3% for low SRG stiffness (i.e., one layer 4 cords/in) to 17% for increased SRG stiffness (i.e., 2 layers of 12 cords/in). The ε_{cc}^p and ε_{ccu}^p values (i.e., the superscript p indicates the predicted values using Equation (3,4)) are compared with the experimental values ε_{cc} and ε_{ccu} (see columns (2) and (3) in

Table 3), respectively. The $\varepsilon_{cc}^{p}/\varepsilon_{cc}$ and $\varepsilon_{ccu}^{p}/\varepsilon_{ccu}$ ratios (columns (5) and (6) in Table 3, respectively) indicate that Equation (3) is conservative, and Equation (4) is less conservative with an exception of columns L2C, which show a larger difference between experimental values ε_{cc} and ε_{ccu}. Given the lateral pressure σ_{lat}, the effective strain of the SRG jacket $\varepsilon_{j,eff}$ is estimated using Equation (1) (see column (7) of Table 3). As seen in Table 3, the predicted values of $\varepsilon_{j,eff}$ are much lower than the material strain capacity (0.025 [24,25]). This is due to the fact that the $\varepsilon_{j,eff}$ corresponds to the average strain along the periphery of the square cross section, and as such, it accounts mainly for the concrete dilation and not the overstrain $\Delta\varepsilon$, which occurs at corners where local effects take place (i.e., stretching due to outwards bending of compression bars). This effect is described explicitly in the Section 4.2.

Table 3. Analytical estimations of the deformation capacity for the SRG confined columns.

	Experimental Data							**Analytical Values**				
Name	f_{cc} MPa	ε_{cc}	ε_{ccu}	σ_{lat}/f_o	$\varepsilon_{cc}^{p}/\varepsilon_{cc}$	$\varepsilon_{ccu}^{p}/\varepsilon_{ccu}$	$\varepsilon_{j,eff}$	$\varepsilon_{s,crit}$ / $f_{s,crit}$ / $\varepsilon_j^{buckl,crit}$	Δf_{cc}	Δf_{ax}	ε_j^{buckl}	$\varepsilon_{ccu}^{buckl}/\varepsilon_{ccu}$
	(1)	(2)	(3)	(4)	(5)	(6)	(7)	(8)	(9)	(10)	(11)	(12)
L1A	31.2	0.0065	0.0098	0.03	0.43	0.36	0.007	0.004 / 540 / 0.013	2.63	3.21	0.013	0.64
L2A	37.9	0.010	0.0116	0.10	0.51	0.98	0.015		5.26	3.21	0.023	1.00
H2A	38.3	0.0155	0.0184	0.11	0.34	0.65	0.005		15.90	3.21	0.014	0.75
L1B	34.0	0.006	0.0105	0.06	0.62	0.45	0.014	0.005 / 540 / 0.013	2.47	0.25	0.022	1.06
L2B	38.2	0.009	0.0113	0.07	0.48	0.64	0.009		4.95	0.25	0.018	0.78
H2B	41.3	0.0145	0.0165	0.14	0.43	1.04	0.006		14.96	0.25	0.015	0.88
L1C	36.3	0.0053	0.0083	0.04	0.61	0.42	0.007	0.007 / 572 / 0.014	2.26	0.0	0.014	0.85
L2C	39.9	0.0073	0.0130	0.13	0.80	1.14	0.016		4.51	0.0	0.023	0.89
H2C	43.5	0.0170	0.0205	0.17	0.41	1.02	0.007		13.65	0.0	0.015	0.71

4.2. Criteria for the Effectiveness of SRG Jacketing in Delaying Bar Buckling

In the present experimental investigation, the application of SRG jackets to RC columns with sparsely spaced stirrups managed to delay but not to preclude buckling of compression reinforcement. According to the mechanics of longitudinal bars embedded in concrete prismatic members, when the bar reaches critical conditions (i.e., instability), it bends laterally to maintain compatibility with the increasing axial strain of the supporting concrete core [4]. Therefore, the concrete core becomes overstressed, and crushing occurs. The critical axial concrete strain of the SRG confined columns is in direct relationship with the mobilized lateral confining pressure. At the same time, the longitudinal bar buckles symmetrically at a stress $f_{s,crit}$ which is related to the available s/D_b ratio [8,12,23,29,32,33]:

$$\frac{s}{D_b} = \Psi\sqrt{\frac{E_{hi}}{f_{s,crit}}} \tag{5}$$

where ψ accounts for the buckling length; $\psi = \pi/4$ when assuming a bar of pinned ends as in the case of yielded ties of poor anchorage ends and $\psi = \pi/2$ of fixed ends as in the case of stiff ties of good anchorage conditions. In the present study, since stirrups are of small diameter (6 mm) and yielded at corners, it is considered $\psi = \pi/4$. The term E_{hi} is the tangent modulus of steel at point ($\varepsilon_{s,crit}$, $f_{s,crit}$) into the hardening branch of the stress–strain relationship (see Figure 8a), defined as per Equation (A2) in Appendix A [2,4].
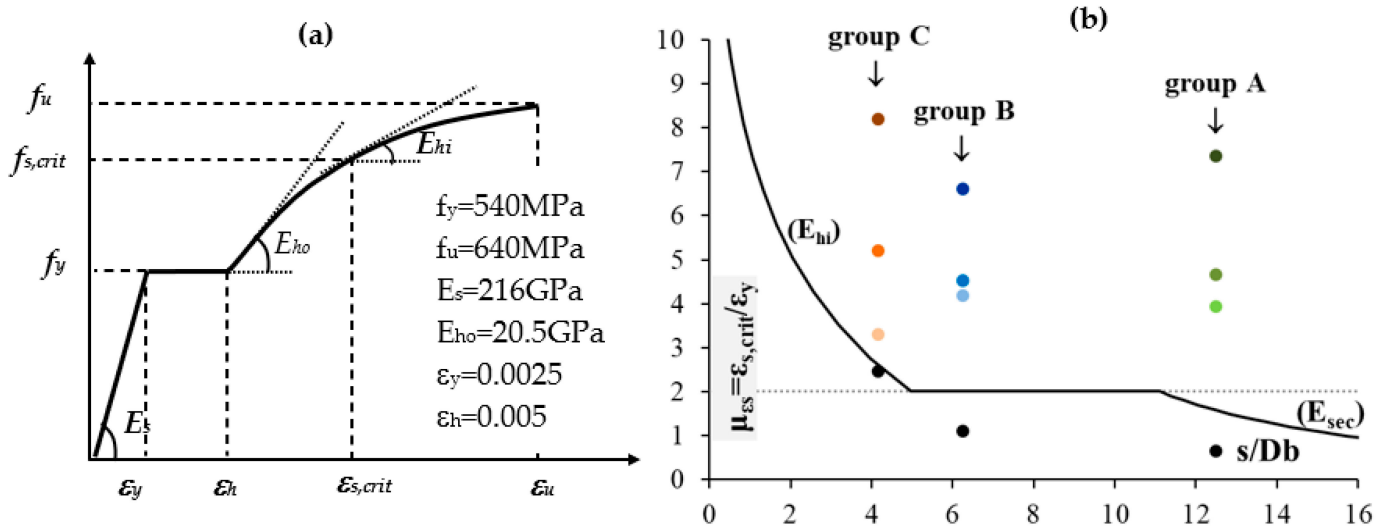
Figure 8. (**a**) Bar stress–strain diagram and (**b**) compressive strain ductility, $\mu_{\varepsilon s}$, versus stirrup spacing s/D_b for the longitudinal reinforcement used in the tests (dots refer to experimental values of $\mu = \varepsilon_{ccu}/\varepsilon_y$).

Equation (5) is also used when steel is into its plateau of zero stiffness, as E_{hi} in Equation (5) is taken equal to the secant modulus $E_{sec} = f_y/\varepsilon_{s,crit}$, with $\varepsilon_{s,crit}$ ranges between ε_y and ε_h. The strain values at yielding, at the end of the yielding plateau and at ultimate (ε_y, ε_h and ε_u, respectively), along with the stress values at yielding and ultimate (f_y and f_u, respectively), for the longitudinal reinforcement used in this study appear in Figure 8a. Note that the term $\varepsilon_{s,crit}$ corresponds to the axial strain at which the bar becomes unstable.

For the post-elastic stress–strain law of the longitudinal bars used in the tests (Figure 8a), the bar compressive strain ductility, $\mu_{\varepsilon s} = \varepsilon_{s,crit}/\varepsilon_y$, is plotted against the ratio s/D_b in Figure 8b; in this buckling curve, the horizontal jump occurs at strain $\varepsilon_{s,crit}$ equal to ε_h as a result of the difference in E_{ho} and E_{sec} at that strain. Additionally, the experimental values (the average of identical specimens was considered) of the columns' compressive strain ductility $\mu = \varepsilon_{ccu}/\varepsilon_y$ are plotted (depicted in circular dots in Figure 8b). The position of the data points relative to the buckling curve denotes (a) when the data points fall below the curve and $\mu_{\varepsilon s} < 1$, then failure occurs due to elastic buckling; (b) when the data points fall under the curve and $\mu_{\varepsilon s} > 1$, then failure occurs due to buckling with steel being into its plateau of zero stiffness—apparently cases (a) and (b) correspond to RC columns with poor reinforcement detailing representative of the old construction practice; (c) when the data points fall on the curve branch denoted by (E_{hi}) in Figure 8b, then failure happens owing to buckling with steel being into the hardening region and the concrete core being unable to undertake the load released by the buckled bars [2]; and (d) when the data points are over the curve and $\mu = \varepsilon_{s,crit}/\varepsilon_y > \varepsilon_h/\varepsilon_y$, then buckling is postponed occurring at higher deformation level due to the efficiency of the confined concrete to undertake the load realised by the buckled bars.

With reference to Figure 8b, the control specimens (black circles) failed near or below yielding of longitudinal reinforcement except for Group C, which coincided with the buckling curve at strain ductility 2.7. In all other cases, SRG jacketing managed to provide the necessary overstrength to the confined concrete core to successfully undertake the released load by the buckled bars (core and bars act as springs in parallel during compression) and to delay failure due to buckling. For the SRG specimens that are placed above the curve of Figure 8b, the following analysis is carried out.

Upon attainment of bar critical strain $\varepsilon_{s,crit} > \varepsilon_y$ ($\varepsilon_{s,crit|A} = 1.5\varepsilon_y$, $\varepsilon_{s,crit|B} = 2\varepsilon_y$ and $\varepsilon_{s,crit|C} = 2.7\varepsilon_y$, see Figure 8b), the corresponding lateral strain of the SRG jacket due

to concrete core dilation $\varepsilon_j^{dil,crit}$ is approximated by considering the apparent Poisson ν as follows:

$$\varepsilon_j^{dil,crit} = \nu\varepsilon_{s,crit} \tag{6}$$

Values for ν for low-to-medium confinement range between 0.5 and 1. At the corners, the jacket is stretched locally by a strain amount $\Delta\varepsilon_{j,ch}^{crit}$ to accommodate the lateral deflection w of the buckled bar. Expressed in polar coordinates, the local hoop strain $\Delta\varepsilon_{j,ch}^{crit}$ is defined as the tangential strain of a thick cylinder of radius $R_{ch} = r + 0.5D_b$ where r is the radius of chamfered specimen corners [12]:

$$\Delta\varepsilon_{j,ch}^{crit} = w/(r + 0.5D_b) \tag{7}$$

At corners, the total strain of the jacket is the sum of Equations (6) and (7) with upper limit being the strain capacity of the jacket $\varepsilon_{ju} = 0.025$ as

$$\varepsilon_{ju} = \varepsilon_j^{dil,crit} + \Delta\varepsilon_{j,ch}^{crit} = \nu\varepsilon_{s,crit} + \Delta\varepsilon_{j,ch}^{crit} \tag{8}$$

Assuming symmetric outwards buckling for the four corner bars, then the mean lateral strain of the jacket calculated over the straight part of the specimen side b_s (here b_s = b − 2r = 200 − 2 × 25 = 150 mm) is $\Delta\varepsilon_j^{crit} = 2w/b_s$, which along with Equations (7) and (8) results in

$$\Delta\varepsilon_j^{crit} = 2\Delta\varepsilon_{j,ch}^{buckl}(r + 0.5D_b)/b_s = 2(\varepsilon_{ju} - \nu\varepsilon_{s,crit})(r + 0.5D_b)/b_s \tag{9}$$

The total mean lateral strain of the jacket upon bar instability by also considering concrete core dilation is

$$\varepsilon_j^{buckl,crit} = \varepsilon_j^{dil,crit} + \Delta\varepsilon_j^{crit} = \nu\varepsilon_{s,crit} + 2(\varepsilon_{ju} - \nu\varepsilon_{s,crit})(r + 0.5D_b)/b_s \tag{10}$$

Equation (9) defines the strain reserve of the jacket upon buckling which corresponds to axial strength reserve of the encased concrete, Δf_{cc}, from Equations (1) and (2) as follows [12]:

$$\Delta f_{cc} = 3\Delta\sigma_{lat} = 3\alpha^{SRG}\rho_v^{SRG}E_f(\varepsilon_{ju} - \nu\varepsilon_{s,crit})(r + 0.5D_b)/b_s \tag{11}$$

As the bars become unstable, they transfer to the encased concrete core overload Δf_{ax} equal to

$$\Delta f_{ax} = (f_{s,crit} - f_{s,res})\frac{As}{(A_{gross} - A_s)}, \quad f_{s,res} = 6f_y/\left(\frac{s}{D_b}\right) \tag{12}$$

where $f_{s,res}$ is the bar residual capacity at an axial strain $\varepsilon \geq \varepsilon_{s,crit}$. For the conservatism of the estimations from Equations (9)–(11), parameter ν is taken equal to unit. Based on [3], an arrangement of $s/D_b < 5$ enables a compression bar to develop a stress–strain response identical to the tensile one. This implies that bars after critical conditions continue to develop stress due to compression and do not release load to the concrete core, and thus, $f_{s,res} = 0$; this is valid for the group C of the present study. If the overload on the bar, represented by Δf_{ax}, exceeds the strength reserve of the core, Δf_{cc}, failure caused by buckling is expected to occur immediately. However, if the overload does not surpass the strength reserve, the risk of buckling-induced failure is mitigated, allowing the core to utilize its complete axial strain capacity, $\varepsilon_{ccu}^{buckl}$, at higher strain levels. In the latter case, the mean lateral strain of the jacket ε_j^{buckl} is described by Equation (10) where $\varepsilon_j^{dil,crit}$ is substituted by $\varepsilon_{j,eff}$ calculated by Equation (1) (see Section 4.1). The relationship between the total mean jacket lateral strain, ε_j^{buckl}, and the associated axial strain capacity, $\varepsilon_{ccu}^{buckl}$, is defined by adopting the Poisson ratio ν_u from $\varepsilon_j^{buckl} = \nu_u\varepsilon_{ccu}^{buckl}$. When the reserve is close to the overload ($\Delta f_{cc} - \Delta f_{ax} < 5\ MPa$), the ν_u can be considered equal to 0.5, else 1.

Table 3 summarizes the analytical estimations of (i) the SRG jacket mean strain upon attainment of critical conditions for the compression reinforcement (column 8) that is lower than the nominal strain capacity, $\varepsilon_{ju} = 0.025$; (ii) the concrete core reserve and the overload (columns 9–10); their comparison reveals than only one case fails upon critical conditions (L1A), and for all other cases, the jacket is able to develop higher strain (column 11) than the critical value $\varepsilon_j^{buckl,crit}$; the ε_j^{buckl} values are close to the nominal strain capacity given by the manufacturer (0.015); and (iii) the column axial strain capacity $\varepsilon_{ccu}^{buckl}$ when it is compared with the experimental one (column 12) shows better agreement than of the column (6) where the predicted values from Equation (4) are characterized by strong conservatism. The satisfactory predictivity of the proposed methodology allows for design purposes to define the effective strain of the SRG jacket $\varepsilon_{j,eff}$ as well as the axial deformation capacity of the confined column in compression $\varepsilon_{ccu}^{buckl}$.

5. Conclusions

The effectiveness of SRG jackets in delaying bar buckling in substandard RC columns under uniaxial compression was experimentally investigated. The study involved applying single- and double-layered SRG jackets with varying axial stiffness to 18 out of the 24 RC columns. Among the 18 specimens, 12 were intentionally designed to be prone to premature buckling, representing older construction practices, with a slenderness ratio (s/D_b) of 6.25 and 12.5. The remaining columns complied with current code requirements. The different jacket schemes were distinguished based on the fabric density and the number of plies used. These variations included jackets with 4 cords/in and one or two layers, as well as jackets with 12 cords/in and two layers. The following conclusions are drawn:

(1) All the unconfined columns (control specimens) failed due to buckling of the longitudinal compression reinforcement developing similar axial strength (around 30 MPa, which coincides with the cylinder concrete compressive strength) regardless of the s/D_b values. Especially for the well-detailed specimens of group C with the dense stirrups, this implies that the stirrups' confining action does not offer any gain in the axial compressive strength. For those cases where $s/D_b > 6$ (groups A, B), the axial strain at the initiation of strength degradation was lower than the yielding threshold of the compression bars, implying elastic buckling of the internal reinforcement. Only the well-detailed specimens C developed a marginal ductility (double of the yielding threshold of the compression bars), implying inelastic buckling.

(2) The majority of the SRG-jacketed columns experienced progressive failure until advanced state of axial deformation due to inelastic bar buckling. The cords ruptured predominantly at the middle height of the specimens, accompanied by progressive debonding of the textile material at the anchorage zone. When two-layered SRG jackets were applied to the specimens, cord rupture was observed in both layers.

(3) Columns with poor detailing ($s/D_b > 6$, smooth stirrups with improper anchoring) were benefitted by a light, single-layered, 4 cords/in SRG jacket mainly as per the increase of the axial strain at the initiation of strength degradation over double the yielding threshold, thus approximating the response of the well-detailed unconfined C specimens. Moreover, this SRG configuration offered (a) a milder post-strength response in comparison to the unconfined C specimens and (b) a marginal increase of axial strength (10–15%). The also easily applicable double-layered 4 cords/in SRG jacketing had the potential to increase the concrete axial strength by 20–30% attaching a more ductile response in comparison to the lighter jacket ($\varepsilon_{cc}/\varepsilon_y = 4$ versus 2.5). Moreover, the denser (12 cords/in), two-layered SRG jacket provided an additional 10% increase in strength whereas the axial strain ductility reached a minimum of 6. A note of caution is that in the case of the high density and stiffness jacket (12 cords/in, two-layered jacket), the design engineer should assess whether its advantages outweigh the challenges posed by the application difficulties (mortar penetration, fitting at the rounded corners of the member). The evaluation of these findings denotes that the SRG jacketing is a promising method for enhancing the behaviour

of old-type RC columns by delaying bar buckling and thus enabling the members to achieve greater strength and deformation capacity.

(4) The analysis of experimental data, following the guidelines presented in Chapter 8 of the fib Bulletin 90 [23] for FRP jacketing and by also considering a proposed model that accounts for the impact of bar buckling on the deformation of the SRG jacket, demonstrates satisfactory predictions for columns with varying levels of detailing. More specifically, the SRG jacket mean strain upon attainment of critical conditions for the compression reinforcement is lower than the material nominal strain capacity, $\varepsilon_{ju} = 0.025$. At this stage, the concrete core axial strength reserve due to SRG confinement exceeds the overload released by the bars as they tend to bend outwards, thus enabling the jacket to be mobilized up until the conservative, nominal strain capacity given by the material manufacturer (0.015). The satisfactory predictivity of the proposed methodology allows for design purposes to define the effective, usable strain of the SRG jacket $\varepsilon_{j,eff}$ as well as the axial deformation capacity of the confined column in compression.

The relevance of this research findings for practical implementation may sum up as follows: the number of SRG jacket layers is determined by two conditions. Firstly, it aims to demonstrate the effectiveness in enhancing either the deformation capacity or both the deformation capacity and strength. Based on the current results, an engineer can select the appropriate jacket configuration that suits the rehabilitation needs of the structure. Secondly, jacketing of high moment regions, such as the plastic hinge of columns, is a localized measure that needs to be combined with global measures aimed at reducing seismic demand in those areas, such as increasing stiffness. Hence, if demand is moderate, then a jacket of few layers can ensure member structural integrity. In case of columns designed to meet current seismic provisions, it may be necessary to use an SRG jacket in case of alterations in the building's use (i.e., importance factor [29]).

Appendix A

Auxiliary Equations used in the proposed methodology.

Explanation	Formula
Equation (A1): confinement effectiveness factor for the SRG jacket (r = 25 mm, b = h = 200 mm)	$\alpha^{SRG} = 1 - \frac{(b-2r)^2 + (h-2r)^2}{3bh}$
Equation (A2): Description of steel stress–strain relationship into the hardening branch and the associated tangent modulus E_{hi}, as per [2,4] and Figure 8a:	$f_{s,crit} = f_u + (f_y - f_u)\left(\frac{\varepsilon_u - \varepsilon_{s,crit}}{\varepsilon_u - \varepsilon_h}\right)^p$ $p = E_{ho}\frac{\varepsilon_u - \varepsilon_h}{f_u - f_y}$ $E_{hi} = E_{ho}\left(\frac{\varepsilon_u - \varepsilon_{s,crit}}{\varepsilon_u - \varepsilon_h}\right)^{p-1}$

References

1. FIB. FIB Bulletin 24 (2003). *Seismic Assessment of Retrofit of Reinforced Concrete Buildings. State of the Art Report by TG 7.1*; Federation International du Béton (FIB): Lausanne, Switzerland, 2003; ISBN 1562-3610.
2. Mau, S. Effect of tie spacing on inelastic buckling of reinforcing bars. *ACI Struct. J.* **1990**, *87*, 671–677.
3. Monti, G.; Nuti, C. Nonlinear cyclic behavior of reinforcing bars including buckling. *J. Struct. Eng.* **1992**, *118*, 3268–3284. [CrossRef]
4. Pantazopoulou, S. Detailing for reinforcement stability in RC members. *J. Struct. Eng.* **1998**, *124*, 623–632. [CrossRef]
5. Yalcin, C.; Saatcioglu, M. Inelastic analysis of reinforced concrete columns. *Comput. Struct.* **2000**, *77*, 539–555. [CrossRef]
6. Maalej, M.; Tanwongsval, S.; Paramasivam, P. Modelling of rectangular RC columns strengthened with FRP. *Cem. Concr. Compos.* **2003**, *25*, 263–276. [CrossRef]
7. Bournas, D.A.; Triantafillou, T.C. Bar buckling in rc columns confined with composite materials. *J. Compos. Constr.* **2011**, *15*, 393–403. [CrossRef]
8. Pantazopoulou, S.J.; Tastani, S.P.; Thermou, G.E.; Triantafillou, T.; Monti, G.; Bournas, D.; Guadagnini, M. Background to European seismic design provisions for the retrofit of R.C. elements using FRP materials. *Fib. Struct. Concr. J.* **2016**, *17*, 133–305.
9. Bournas, D.A.; Lontou, P.V.; Papanicolaou, C.G.; Triantafillou, T.C. Textile-Reinforced Mortar versus Fiber-Reinforced Polymer Confinement in Reinforced Concrete Columns. *ACI Struct. J.* **2007**, *104*, 740–748.
10. Manos, G.C.; Kourtides, V. Retrofitting of long rectangular R/C cross-sections with partial confinement employing carbon fiber reinforcing plastics. In Proceedings of the FRPRCS-8 Conference, Patras, Greece, 16–18 July 2007; p. 128.
11. Manos, G.C.; Katakalos, K. The use of fiber reinforced plastic for the repair and strengthening of existing reinforced concrete structural elements damaged by earthquakes. In *Fiber Reinforced Polymers—The Technology Applied for Concrete Repair*; Masuelli, M.A., Ed.; Intechopen: London, UK, 2013; ISBN 978-953-51-0938-9.
12. Tastani, S.; Pantazopoulou, S.; Zdoumba, D.; Plakantaras, V.; Akritidis, E. Limitations of FRP jacketing in confining old-type reinforced concrete members in axial compression. *J. Compos. Constr.* **2006**, *10*, 13–25. [CrossRef]
13. Thermou, G.E.; Pantazopoulou, S.J. Fiber reinforced polymer retrofitting of substandard RC prismatic members. *J. Compos. Constr.* **2009**, *13*, 535–546. [CrossRef]
14. Thermou, G.E.; Pantazopoulou, S.J. Metallic fabric jackets: An innovative method for seismic retrofitting of substandard RC prismatic members. *Fib. Struct. Concr. J.* **2007**, *8*, 35–46. [CrossRef]
15. Thermou, G.E.; Papanikolaou, V.K.; Hajirasouliha, I. Structural performance of RC columns retrofitted with steel-reinforcedgrout jackets under combined axial and lateral loading. *Eng. Struct.* **2021**, *245*, 11294. [CrossRef]
16. Kennedy-Kuiper, R.C.S.; Wakjira, T.G.; Alam, M.S. Repair and Retrofit of RC Bridge Piers with Steel-Reinforced Grout Jackets: An Experimental Investigation. *ASCE J. Bridge Eng.* **2022**, *27*, 04022067. [CrossRef]
17. Bencardino, F.; Nisticò, M. Behavior under Repeated Loading of RC Beams Externally Strengthened in Flexure with SRG Systems. *Materials* **2023**, *16*, 1510. [CrossRef] [PubMed]
18. Ombres, L.; Verre, S. Influence of the Strengthening Configuration on the Shear Capacity of Reinforced Concrete Beams Strengthened with SRG (Steel-Reinforced Grout) Composites. *Fibers* **2022**, *10*, 57. [CrossRef]
19. Thermou, G.E.; Katakalos, K.; Manos, G. Influence of the loading rate on the axial compressive behavior of concrete specimens confined with SRG jackets. In Proceedings of the ECCOMAS Thematic Conference COMPDYN, Kos, Greece, 12–14 June 2013; p. 1482.
20. Thermou, G.E.; Katakalos, K.; Manos, G. Concrete confinement with steel-reinforced grout jackets. *Mater. Struct.* **2015**, *48*, 1355–1376. [CrossRef]
21. Thermou, G.E.; Katakalos, K.; Manos, G. Influence of the cross section shape on the behaviour of SRG-confined prismatic concrete specimens. *Mater. Struct.* **2016**, *49*, 869–887. [CrossRef]
22. Katsamakas, A.A.; Papanikolaou, V.K.; Thermou, G.E.; Katakalos, K. Experimental and numerical investigation of the uniaxial compression behavior of SRG-Jacketed R/C columns. *Elsevier Struct.* **2022**, *4*, 603–617. [CrossRef]
23. FIB. *FIB Bulletin 90, Externally Applied FRP Reinforcement for Concrete Structures. Technical Report by Task Group 5.1*; Federation International du Béton (FIB): Lausanne, Switzerland, 2019; ISBN 978-2-88394-131-1.
24. Mazzuca, S.; Hadam, H.A.; Ombres, L.; Nanni, A. Mechanical Characterization of Steel-Reinforced Grout for Strengthening of Existing Masonry and Concrete Structures. *ASCE J. Mater. Civ. Eng.* **2019**, *31*, 04021467. [CrossRef]
25. Thermou, G.E.; De Santis, S.; de Felice, G.; Alotaibi, S.; Roscini, F.; Hajirasouliha, I.; Guadagnini, M. Bond behaviour of multi-ply steel reinforced grout composites. *Constr. Build. Mater.* **2021**, *305*, 124750. [CrossRef]
26. Ombres, L.; Verre, S. Experimental and Numerical Investigation on the Steel Reinforced Grout (SRG) Composite-to-Concrete Bond. *J. Compos. Sci.* **2020**, *4*, 182. [CrossRef]
27. Toutanji, H.; Han, M.; Ghorbel, E. Interfacial Bond Strength Characteristics of FRP and RC Substrate. *ASCE J. Compos. Constr.* **2012**, *16*, 35–46. [CrossRef]
28. Pellegrino, C.; Modena, C. Analytical Model for FRP Confinement of Concrete Columns with and without Internal Steel Reinforcement. *ASCE J. Compos. Constr.* **2010**, *14*, 693–705. [CrossRef]
29. Tastani, S.; Pantazopoulou, S. Detailing procedures for seismic rehabilitation of reinforced concrete members with fiber reinforced polymers. *Eng. Struct.* **2008**, *30*, 450–461. [CrossRef]

30. *EN1998-1-2004*; Eurocode 8, Design of Structures for Earthquake Resistance—Part I: General Rules, Seismic Actions and Rules for Buildings. European Committee for Standardization (CEN): Brussels, Belgium, 2004.
31. Richart, F.; Brandtzaeg, A.; Brown, R. *A Study of Failure of Concrete under Combined Compressive Stresses*; Engineering Experiment Station, University of Illinois, Urbana: Urbana, IL, USA, 1928; p. 185.
32. Priestley, M.; Seible, F.; Calvi, M. *Seismic Design and Retrofit of Bridges*; Wiley: New York, NY, USA, 1996.
33. Papia, M.; Russo, G.; Zingone, G. Instability of longitudinal bars in RC columns. *J. Struct. Eng.* **1988**, *114*, 445–461. [CrossRef]